Published in final edited form as:
Development. 2007 February ; 134(3): 545–555. doi:10.1242/dev.02764.

Controlled overexpression of Pax6 in vivo negatively autoregulates the *Pax6* locus, causing cell-autonomous defects of late cortical progenitor proliferation with little effect on cortical arealization

Martine Manuel[1,*], **Petrina A. Georgala**[1], **Catherine B. Carr**[1], **Simon Chanas**[2], **Dirk A. Kleinjan**[3], **Ben Martynoga**[1], **John O. Mason**[1], **Michael Molinek**[1], **Jeni Pinson**[1], **Thomas Pratt**[1], **Jane C. Quinn**[1], **T. Ian Simpson**[1], **David A. Tyas**[1], **Veronica van Heyningen**[3], **John D. West**[2], and **David J. Price**[1]

[1]Genes and Development Group, Centres for Integrative Physiology and Neuroscience Research, Hugh Robson Building, George Square, University of Edinburgh, Edinburgh EH8 9XD, UK

[2]Division of Reproductive and Developmental Sciences, Genes and Development Group, Centres for Integrative Physiology and Reproductive Biology, Hugh Robson Building, George Square, University of Edinburgh, Edinburgh EH8 9XD, UK

[3]MRC Human Genetics Unit, Western General Hospital, Edinburgh EH4 2XU, UK

Abstract

Levels of expression of the transcription factor Pax6 vary throughout corticogenesis in a rostro-lateral^{high} to caudo-medial^{low} gradient across the cortical proliferative zone. Previous loss-of-function studies have indicated that Pax6 is required for normal cortical progenitor proliferation, neuronal differentiation, cortical lamination and cortical arealization, but whether and how its level of expression affects its function is unclear. We studied the developing cortex of PAX77 YAC transgenic mice carrying several copies of the human *PAX6* locus with its full complement of regulatory regions. We found that PAX77 embryos express Pax6 in a normal spatial pattern, with levels up to three times higher than wild type. By crossing PAX77 mice with a new YAC transgenic line that reports Pax6 expression (DTy54), we showed that increased expression is limited by negative autoregulation. Increased expression reduces proliferation of late cortical progenitors specifically, and analysis of PAX77↔wild-type chimeras indicates that the defect is cell autonomous. We analyzed cortical arealization in PAX77 mice and found that, whereas the loss of Pax6 shifts caudal cortical areas rostrally, Pax6 overexpression at levels predicted to shift rostral areas caudally has very little effect. These findings indicate that Pax6 levels are stabilized by autoregulation, that the proliferation of cortical progenitors is sensitive to altered Pax6 levels and that cortical arealization is not.

Keywords

Pax6; Cortex; Overexpression; Autoregulation; Proliferation; Neurogenesis; Lamination; Regionalization; Thalamocortical; Chimeras

[*] Author for correspondence (e-mail:Martine.Manuel@ed.ac.uk).

Europe PMC Funders Author Manuscripts

INTRODUCTION

The complexity of brain structure and function is established through the generation of numerous and frequently subtle differences among progenitor cells and the neurons that they produce. Molecular differences between cells in the embryonic nervous system are detectable from its inception and arise as cells are exposed to different levels of morphogens released by surrounding signalling centres. These morphogens determine the levels of expression of key transcription factors that pattern the nervous system, creating domains that express characteristic combinations of transcription factors specifying their morphologies and functions (Kerszberg, 1999; Neumann and Cohen, 1997; Tabata and Takei, 2004; Yucel and Small, 2006). The potential of a limited set of transcription factors to direct the generation of an enormous diversity of neuronal phenotypes might be enhanced greatly if different levels of transcription factors cause different developmental outcomes. If levels of expression are important, then two predictions can be made: (i) developing neurons should contain mechanisms to stabilize levels of expression of transcription factors in the face of altering exposure to environmental signals as the embryo grows and changes; and (ii) neurogenesis should be affected if levels of transcription factor expression are altered. Here, we tested these predictions for the transcription factor Pax6.

Mice homozygous for a loss-of-function mutation of *Pax6* lack eyes and nasal structures, and die at birth with serious brain abnormalities, including forebrain patterning and growth defects (Bishop et al., 2000; Bishop et al., 2002; Estivill-Torrus et al., 2002; Grindley et al., 1997; Hill et al., 1991; Hogan et al., 1986; Kroll and O'Leary, 2005; Mastick et al., 1997; Muzio et al., 2002; Pratt et al., 2000; Schmahl et al., 1993; Stoykova et al., 1996; Warren and Price, 1997). In normal mice, corticogenesis occurs from E10.5 to E17.5 by a process of progenitor proliferation in the ventricular zone (VZ) followed by migration of neural precursors to the overlying cortical plate. *Pax6* is expressed in the VZ throughout corticogenesis (Caric et al., 1997; Estivill-Torrus et al., 2002; Walther and Gruss, 1991) and is implicated in progenitor proliferation, migration, differentiation, lamination and arealization (Bishop et al., 2000; Estivill-Torrus et al., 2002; Heins et al., 2002; Schuurmans et al., 2004; Tarabykin et al., 2001). Previous studies identified a reduced progenitor population and defective differentiation as primary defects resulting from the loss of Pax6 (Heins et al., 2002; Quinn et al., 2006).

Most studies on the functions of Pax6 in brain development have studied the consequences of its removal. Whether the level at which it is expressed in the brain is important is unclear, although its expression in a gradient in the cortex suggests that it might be. Levels of expression in the eye are crucial, with both reduced and increased gene dosage causing defects in development (Schedl et al., 1996). Here, we tested whether increased levels of Pax6 affect cortical progenitor proliferation, cortical lamination and cortical arealization using the PAX77 mouse line produced by Schedl et al. (Schedl et al., 1996). In addition to their two endogenous *Pax6* alleles, mice hemizygous for the *PAX77* transgene carry five to seven copies of the human *PAX6* locus, including its upstream and downstream regulatory regions (the mouse and human Pax6 proteins are identical). The *PAX77* transgene is functional, as demonstrated by its ability to rescue the eye and brain defects in mice carrying loss-of-function mutations of *Pax6* (Schedl et al., 1996).

MATERIALS AND METHODS

Mice

PAX77 hemizygous mice (Schedl et al., 1996), designated *PAX77*$^{+}$, carry five to seven copies of a 420 kb human *PAX6* YAC (Y593) with all copies integrated at the same locus. We refer to the array of integrated YAC Y593 copies as the *PAX77* transgene. PAX77

homozygous mice, designated *PAX77*$^{+/+}$, carry 10-14 copies of human *PAX6* and were genotyped by fluorescent in situ hybridization using the Fat5 probe (Schedl et al., 1996). The PAX77 line was maintained on a CD1 background. The morning of the vaginal plug was deemed E0.5. The first 24 hours after birth was deemed P0. Animal care followed institutional guidelines and UK Home Office regulations.

Western blots

For each protein sample, two E12.5 telencephalons of the same genotype were combined and lysed in TENT buffer (20 mM Tris-HCl, pH 8.0; 2 mM EDTA; 150 mM NaCl; 1% (v/v) Triton-X100). Subsequent processing followed Pinson et al. (Pinson et al., 2006), using anti-Pax6 serum 13 (1:200; from S. Saule, Institut Curie, Paris, France) (Carriere et al., 1993) and anti b-actin (1:5000; Sigma). Densities of bands on X-ray films were quantified with a GS-710 densitometer and Quantity One software (BioRad).

Autoregulation of Pax6

We generated reporter transgenic mice containing one copy of a modified version of the *PAX6*-containing YAC used to generate the PAX77 line. The modified YAC (Y1123) contains the upstream and downstream regulatory regions sufficient to recapitulate full *PAX6* expression, but the *PAX6* gene is rendered non-functional by the insertion of a tau-green fluorescent protein (tau-GFP) reporter construct (Tyas et al., 2006). Expression of tau-GFP from Y1123 in these mice, named DTy54, reports faithfully the sites and levels of endogenous *Pax6* expression (Tyas et al., 2006). Here, we studied the expression from Y1123 in *Pax6*$^{+/+}$, *Pax6*$^{Sey/Sey}$ (designated *Pax6*$^{-/-}$) or *PAX77*$^{+}$ embryos. Embryos were fixed (4% paraformaldehyde) and embedded in 4% low-melting-point agarose. Vibratome sections (200 μm) were counterstained with TOPRO3 (Molecular Probes, NL) and imaged (Leica confocal microscope). To prepare isolated cells, heads from E14.5 *Pax6*$^{+/+}$, *Pax6*$^{-/-}$ or PAX77 embryos also carrying Y1123, or from wild-type embryos were dissociated (Papain Dissociation System, Worthington Biochemical). Cells were analyzed on a Beckman-Coulter XL flow cytometer (10,000-20,000 cells per sample).

Quantitative reverse transcription PCR

Telencephalic cDNA samples were collected from E14.5 wild-type or *PAX77*$^{+}$ embryos. Quantitative reverse transcription PCR (qRT-PCR) used the following primer pairs: mouse *Pax6* (5′-AACACCAACTCCATCAGTTC-3′ and 5′-ATCTGGATAATGGGTCCTCT-3′; 153 bp product) and *18S* ribosomal RNA (5′-GTGGAGCGATTTGTCTGGTT-3′ and 5′-CAAGCTTATGACCCGCACTT-3′; 321 bp product). qRT-PCR was performed using Qiagen Quantitect SYBR Green PCR kit (Qiagen, USA) and a DNA Engine Opticon Continuous Fluorescence Detector (GRI, UK). The abundance of each transcript in the original RNA sample was extrapolated from PCR reaction kinetics using Opticon software.

Cortical progenitor proliferation

E12.5 or E15.5 pregnant females were sacrificed 1 hour after injection with 200 μl of 10 mg/ml bromodeoxyuridine (BrdU, Sigma; in 0.9% NaCl, intraperitoneal). Wax sections (10 μm) were immunostained with anti-BrdU or anti-phosphorylated histone H3. Cells were counted in 100 μm-wide sampling boxes in the VZ and subventricular zone (SVZ) of the rostral, central and caudal cortex of three wild-type and three *PAX77*$^{+}$ embryos. Each count was repeated on three to five non-adjacent sections from each embryo for BrdU analysis and on 10-19 non-adjacent sections for phosphorylated histone H3 analysis.

Cortical layer thickness

A total of three wild-type and three *PAX77*$^{+}$ P7 pups were anesthetized and perfused with 4% paraformaldehyde. Coronal wax sections (10 μm) were stained with cresyl violet. For each brain, the thickness of the cortical layers was measured using the Image Tool software (University of Texas Health Science Centre at San Antonio, San Antonio, TX, USA) on 16-28 non-adjacent sections at equivalent rostral, central and caudal levels.

Chimeric embryos

Chimeras were produced by embryo aggregation (West and Flockhart, 1994). Embryos differed at the *Gpi1* locus (encoding glucose phosphate isomerase) and one of each pair carried a reiterated β-globin *TgN (Hbb-b1)* transgene (abbreviated to *Tg*), identifiable by DNA in situ hybridization (Keighren and West, 1993; Lo, 1986; Lo et al., 1987). Outbred CD1A females (homozygous *Gpi1*$^{a/a}$ CD1 strain mice) were induced to ovulate and were mated to hemizygous *PAX77*$^{+}$ males on a CD1A background to produce *PAX77*$^{+}$ and wild-type embryos, all of which were *Gpi1*$^{a/a}$;*Tg*$^{-/-}$. (C57BL/6×CBA/Ca)F1 females (*Gpi1*$^{b/b}$; *Tg*$^{-/-}$) were induced to ovulate and were mated to 'BTC'-strain males (*Gpi1*$^{b/b}$;*Tg*$^{+/+}$ on a mixed [C57BL/6×CBA/Ca] background) to produce embryos, all of which were wild-type, *Gpi1*$^{b/b}$; *Tg*$^{+/-}$. Chimeras were transferred to pseudopregnant *Gpi1*$^{c/c}$ ('CF1' hybrid strain) females. E16.5 foetuses were dissected into cold PBS, and their limbs and tails were removed and analyzed by GPI1 electrophoresis (West and Flockhart, 1994). Heads were fixed and processed for analysis by in situ hybridization and other body tissues were digested to obtain DNA for PCR genotyping to distinguish PAX77↔wild-type and wild-type↔wild-type chimeras. A total of three to five non-consecutive coronal sections from each chimeric brain were examined for each hemisphere and each region along the anterior-posterior axis. Percentages of Tg^{-} cells were determined by counting numbers of hybridization signals and nuclei in 100 μm-wide boxes. The contribution of *Gpi1*$^{a/a}$ cells to chimeras used here was 42-86%.

To determine proportions of Tg^{-} and Tg^{+} cells in M-phase in PAX77↔wild-type chimeras, β-globin DNA in situ hybridization was followed by immunostaining with anti-phosphorylated histone H3. Nickel was added to the diaminobenzidine visualization solution to obtain a grey precipitate. Cells were counted in 100 μm-wide sampling boxes in the VZ of the rostral cortex of each E16.5 chimeric or wild-type embryo. Each count was repeated on four to five non-adjacent sections. The contribution of *Gpi1*$^{a/a}$ cells to the chimeras used here was 42-57%.

Immunohistochemistry

Processing for Emx2 detection was as described in Mallamaci et al. (Mallamaci et al., 1996), for Ephrin B2 detection was as in Pratt et al. (Pratt et al., 2004) and for all other immunochemistry reactions was as in Martynoga et al. (Martynoga et al., 2005). Immunostaining reactions were performed as in Martynoga et al. (Martynoga et al., 2005), except that antigen retrieval was not necessary for Emx2 detection. Primary antibodies were BrdU (1:200; Becton Dickinson), phosphorylated histone H3 (1:500; Sigma), Pax6 (1:500; DSHB), Emx2 (1:500, a gift from G. Corte, National Institute for Cancer Research, Genova, Italy) and Ephrin B2 (1:500; R&D Systems AF496,). To analyze the cortical Pax6 gradient, a biotinylated secondary antibody was used with Alexa Fluor 488-conjugated streptavidin (Molecular Probes, Inc.). Serial sagittal sections through four cortical hemispheres from wild-type and *PAX77*$^{+/+}$ E12.5 embryos were analyzed (Leica confocal microscope). The fluorescence intensity was quantified on each section in 50 μm×50 μm boxes placed at rostral and caudal cortical poles, and the ratio between the two was calculated. The highest anterior/posterior ratio for each cortical hemisphere was used to give a value for the

maximum steepness of its Pax6 gradient. An average was calculated from all four hemispheres.

In situ hybridization

For *Id2* in situ hybridization, embryos were dissected (cold PBS), fixed overnight (4% paraformaldehyde), wax-embedded and sectioned (10 μm). In situ hybridization was performed (Porteus et al., 1992) using a digoxigenin-labeled anti-sense *Id2* RNA probe (from D. O'Leary, the Salk institute, La Jolla, USA).

Analysis of the cortical barrel field

P7 pups were anesthetized and perfused (4% paraformaldehyde), and cerebral hemispheres were removed, postfixed between slides and then cryoprotected in 30% sucrose. Tangential serial 48 μm frozen sections were obtained and immunostained for serotonin transporter (Watson et al., 2006). Images were captured (Leica DMLB microscope), and linear and area measurements obtained (Image Tool software).

RESULTS

Pax6 protein levels are increased in PAX77 mice

We compared Pax6 protein levels in wild-type, $PAX77^{+}$ and $PAX77^{+/+}$ embryonic brains using western blots (Fig. 1A,B). The two major isoforms of Pax6 - Pax6 (46 kDa) and Pax6(5a) (48 kDa) - were significantly upregulated in $PAX77^{+}$ and $PAX77^{+/+}$ brains compared with wild type (Fig. 1B). The increases were not as great as the increases in the numbers of copies of the gene, and there was no significant difference in the levels of Pax6 and Pax6(5a) between $PAX77^{+}$ and $PAX77^{+/+}$ brains (Fig. 1B). We also analyzed Pax6 expression by immunohistochemistry on sections of E12.5 brains (Fig. 1C-E). The levels of Pax6 appeared higher in both $PAX77^{+}$ and $PAX77^{+/+}$ brains than in wild type. The Pax6 expression pattern in PAX77 brains reproduces that in the wild-type brain without any ectopic sites of expression, and the rostro-lateral^{high} to caudo-medial^{low} gradient of cortical Pax6 expression is conserved (Fig. 1C-E).

Negative autoregulation of the *Pax6* locus

Our finding that Pax6 protein levels do not increase in proportion to gene copy number suggests that a negative autoregulation of the expression of the gene exists. To test this, we examined the expression of tau-GFP from one copy of Y1123 (Material and methods) (Tyas et al., 2006) in embryos that were $Pax6^{+/+}$, $Pax6^{-/-}$ or $PAX77^{+}$ with confocal microscope settings held constant throughout (Fig. 2A-C). The signal was much weaker in the cortex of PAX77 mice (Fig. 2B), and was more intense in $Pax6^{-/-}$ cortex (Fig. 2C), than in wild-type cortex. Previous studies of $Pax6^{-/-}$ brains have shown that, although their morphology is distorted, mutant counterparts of major brain structures are recognizable and *Pax6* mRNA expression is restricted to regions corresponding to Pax6-expressing regions in wild-type mice (Stoykova et al., 1996; Warren and Price, 1997). We found that, in $Pax6^{-/-}$ brains, the expression of tau-GFP from Y1123 is also restricted to these regions; Fig. 2C shows expression limited to dorsal telencephalic cells in mutants, as in wild type (Fig. 2A). Reduced GFP expression in PAX77 embryos and increased expression in $Pax6^{-/-}$ embryos was not confined to the forebrain, but was seen in all regions that express Pax6 (see Fig. S1 in the supplementary material).

Results from flow cytometry on dissociated cells from E14.5 brains are shown in Fig. 2D-H. Data in each histogram in Fig. 2D-G is from a single embryo. Analysis of non-transgenic embryos provided frequency distributions of background fluorescence intensity (Fig. 2D): distributions were similar in different individuals and gate B was set to include an average of

2% of cells (range 1-5%) in a set of 12 samples from non-transgenic embryos. Cells falling within gate B in Y1123 transgenic embryos (Fig. 2E-G) were considered to express tau-GFP. Each frequency distribution shown in Fig. 2D-G was similar to that from all the other embryos of the same genotype (n=4-6 embryos per genotype). For each sample, the average fluorescence intensity of the population of cells within gate B was obtained and data were combined for each genotype group (Fig. 2H); combining values for the median fluorescence intensity of each sample gave the same outcome (data not shown). Embryos of all three genotypes contained populations of GFP-expressing cells, but the average fluorescence intensity of this population was higher on a *Pax6*$^{-/-}$ background (Fig. 2E,F,H) and lower on a PAX77 background (Fig. 2E,G,H). These results indicate that GFP-expressing cells increase their expression levels in the absence of Pax6 proteins, whereas an 1.5- to 3-fold non-ectopic overexpression of Pax6 suppresses GFP expression. We conclude that the level of activity of the Y1123 reporter is inversely related to the level of endogenous Pax6 production.

We carried out qRT-PCR to test whether raised levels of PAX6 protein lowered the expression of *Pax6* mRNA. We found significantly reduced levels of mRNA for mouse *Pax6* in the telencephalon of *PAX77*$^{+}$ E14.5 embryos, to one-third of wild-type levels (Student's t-test, P<0.03; n=3 embryos of each genotype), indicating that Pax6 negatively regulates its own mRNA production and/or stability.

Pax6 overexpression alters cortical progenitor proliferation at late stages of corticogenesis

Previous studies have shown that Pax6 is important in regulating cortical progenitor proliferation and for promoting neurogenesis (Estivill-Torrus et al., 2002; Heins et al., 2002). First, we tested whether overexpression of Pax6 has an effect on cortical-cell proliferation. The proliferative zone of the neocortex contains two populations of progenitors: apical progenitors (APs) undergo mitosis at the ventricular surface and express high levels of Pax6; and basal progenitors (BPs) are derived from APs and divide in the SVZ and basal VZ. Pax6 is downregulated during the transition from AP to BP (Englund et al., 2005). BrdU was used to label cortical progenitors in S-phase of the cell cycle (Fig. 3D,E,G,H), and phosphorylated histone H3 was used as a marker of mitotic progenitors (Fig. 3J,K). We determined the proportion of cells in S-phase (p^{Scells}) in the VZ along the cortex of *PAX77*$^{+}$ and wild-type embryos at E12.5, early in corticogenesis, and were unable to detect any significant difference (Fig. 3A-F). We then determined the p^{Scells} and the density of cells undergoing mitosis (d^{Mcells}) along the cortex of wild-type and *PAX77*$^{+}$ embryos at E15.5, a late stage of corticogenesis. We found a significant reduction of the p^{Scells} (Fig. 3G-I) and the d^{Mcells} (Fig. 3J-L) among APs in the rostral and central cortex of *PAX77*$^{+}$ embryos compared to wild type (Student's t-test, P<0.05). No significant difference was detected in the caudal cortex. Thus, Pax6 overexpression alters the proliferation of rostral and central APs at late stages of corticogenesis, whereas early progenitors seem unaffected. We did not find any significant alteration of p^{Scells} and d^{Mcells} among BPs in the rostral, central and caudal cortex of *PAX77*$^{+}$ embryos compared to wild type (data not shown).

We tested whether overexpression of Pax6 causes an increase in neurogenesis by analyzing the expression of the neuronal marker β-tubulin III in the cortex of wild-type and PAX77 embryos using immunohistochemistry and flow cytometry. We found no difference in the proportions of β-tubulin III-expressing cells in PAX77 embryos compared to wild type (see Fig. S2 in the supplementary material).

Effects of overexpression of Pax6 on late cortical progenitors are cell autonomous

In PAX77 mice, Pax6 levels are increased at all of its sites of expression, and so a late-onset cortical defect might arise as a secondary consequence of defects elsewhere (e.g. PAX77 mice are microphthalmic and may have other as yet undetected extra-cortical abnormalities). We tested whether the defects detected in mutants reflect a requirement for a correct level of Pax6 within cortical progenitors themselves rather than in their environment. To discriminate between these two possibilities, we analyzed foetal chimeras in which the mutant cells have the potential to interact with wild-type cells so that any defects that they retain are therefore more likely to be cell autonomous.

Embryos derived from a wild type×*PAX77*$^{+}$ cross were aggregated to wild-type embryos, carrying the Tg transgene as a marker, to produce control chimeras [wild-type;Tg^{-}↔wild-type;Tg^{+}] or mutant chimeras [*PAX77*$^{+}$;Tg^{-}↔wild-type;Tg^{+}]. Cells derived from the wild-type embryo could be identified, after DNA in situ hybridization against *Tg*, by the presence of a brown spot in the nucleus (Fig. 4A,B). The global percentage of cells derived from each of the two embryos used to generate each chimera was estimated by quantitative analysis of GPI1 isozyme composition of the limbs (West and Flockhart, 1994), with the percentage of the GPI1A isozyme representing the contribution of cells derived from the wild-type×*PAX77*$^{+}$ cross.

We analyzed three control and four mutant chimeras at E16.5 and determined the percentage of Tg^{-} cells in the proliferative zones (VZ and SVZ), the intermediate zone (IZ) and the cortical plate (CP) at rostral, central and caudal positions of each chimeric cortex. For each chimera, the observed contribution of Tg^{-} cells to each cortical region (obsTg^{-}) was compared to the expected contribution of Tg^{-} cells (expTg^{-}) given by the percentage of GPI1A for that chimera. The mean ratio obsTg^{-}:expTg^{-} in the different cortical regions of the control chimeras was always slightly greater than 1 (between 1.08 and 1.23, Fig. 4C-E), reflecting the fact that the brown spot identifying Tg^{+} cells was not always present in the plane of section analyzed, and the number of Tg^{-} cells was therefore slightly overestimated. This applied equally to control and mutant chimeras. Our results showed that the Tg^{-} cells in the mutant chimeras were significantly under-represented in the proliferative zones of the rostral (Student's *t*-test, $P<0.01$), central ($P<0.05$) and caudal ($P<0.05$) cortex compared with the control chimeras (Fig. 4C). The Tg^{-} cells in the mutant chimeras were also significantly under-represented in the IZ of the rostral cortex (Student's *t*-test, $P<0.05$) compared with control chimeras (Fig. 4D). We did not detect any difference in the contribution of Tg^{-} cells to the cortical plate between mutant and control chimeras (Fig. 4E), consistent with there having been no earlier defect in production of postmitotic cells. Overall, these results indicate that, late in corticogenesis, cortical progenitors must express normal levels of Pax6 to contribute normally to the proliferative zones of the cortex.

We tested whether the under-representation of Pax6 overexpressing cells in the cortical proliferative zones of chimeras was due to a cell-autonomous proliferation defect using phosphorylated histone H3 as a marker of mitotic cells (Fig. 4F,G). We compared the average proportion of Tg^{+} and Tg^{-} cells in M-phase (p^{MTg+} and p^{MTg-}, respectively) in the VZ of the rostral cortex of mutant chimeras to the average proportion of cells in M-Phase (p^{Mcells}) in the corresponding region of wild-type embryos. The average proportion of mutant cells in M-phase (p^{MTg-}) in chimeras (0.0123±0.0044 s.e.m., $n=3$) was significantly lower than p^{Mcells} in wild-type embryos (Student's *t*-test, $P<0.03$), indicating that correct levels of Pax6 are required cell-autonomously in order to enable late cortical progenitors to proliferate normally. We found that p^{MTg+} in mutant chimeras (0.0243±0.003 s.e.m., $n=3$) was not significantly different from p^{Mcells} in wild-type embryos (0.0242±0.003 s.e.m., $n=3$), indicating that the presence of Pax6-overexpressing cells does not affect the proliferation of wild-type cortical progenitors in mutant chimeras.

Pax6 overexpression decreases the thickness of superficial cortical layers

The formation of superficial cortical layers occurs during late stages of corticogenesis (Caric et al., 1997). We tested whether the defect in late cortical progenitor proliferation observed in PAX77 embryos results in postnatal lamination defects. We compared the thickness of deep (V and VI) and superficial (II-IV combined) cortical layers and of the marginal zone (future layer I) in *PAX77*$^{+}$ and wild-type brains at P7 (Fig. 5). The thickness of superficial layers II-IV was significantly decreased in the rostral and central PAX77 cortex compared to the wild-type cortex (Student's *t*-test, $P<0.01$, $n=3$ brains of each genotype; Fig. 5C,D). The thickness of deep cortical layers and that of layer I are not significantly altered in the PAX77 cortex. This is consistent with the late cortical progenitor proliferation defects observed in PAX77 embryos.

Cortical arealization is largely unaffected by Pax6 overexpression

Previous work has suggested that *Pax6* plays a crucial role in cortical arealization by conferring rostro-lateral identities to cortical progenitors (Bishop et al., 2000; Bishop et al., 2002; Muzio et al., 2002). The arealization of the neocortex is altered in *Pax6*$^{-/-}$ mice: caudo-medial areas expand while rostro-lateral areas shrink. Moreover, expression of the gene encoding the transcription factor Emx2, which confers caudo-medial identities, is upregulated, suggesting that Pax6 downregulates *Emx2* (Muzio et al., 2002). Accordingly, we predicted that the overexpression of Pax6 would have an opposite effect on cortical regionalization (i.e. the downregulation of *Emx2* and a caudo-medial shift of rostro-lateral areas at the expense of caudo-medial regions) (Fig. 6). To address the issue of how the observed overexpression of Pax6 in the brains of PAX77 mice [1.5- to 2-fold and 3-fold for Pax6 and Pax6(5a), respectively; Fig. 1] would be expected to impact cortical regionalization, we measured the steepness of the cortical Pax6 gradient by quantitative comparison of fluorescent Pax6 immunoreactivity between rostral and caudal cortical poles of each of a series of sagittal sections (Materials and methods). The fluorescence intensity was used as an indication of relative Pax6 expression levels. We found that the average ratio between rostral and caudal Pax6 levels is 3.37 (±0.26 s.e.m., $n=4$) in the wild-type cortex and 4.16 (±0.4 s.e.m., $n=4$) in the *PAX77*$^{+}$ cortex (not significantly different, Student's *t*-test). As shown in Fig. 6A, this indicates that the overall steepness of the Pax6 gradient is increased in the cortex of PAX77 embryos and the increase of Pax6 levels observed in the brains of PAX77 transgenic embryos would be expected to displace anterior cortical regions that normally express the highest levels of Pax6 to the posterior pole of the cortex.

To search for defects in cortical arealization in PAX77 mice, we first analyzed the expression of *Emx2*, ephrin B2 and *Id2*, because their expression is normally restricted or graded across the developing cortex of embryos (Bishop et al., 2000; Bishop et al., 2002; Mallamaci et al., 1998; Muzio et al., 2002; Rubenstein et al., 1999). Emx2 is normally expressed in a caudo-medial^{high} to rostro-lateral^{low} gradient in the embryonic cortex and this gradient is conserved in *PAX77*$^{+}$ (and *PAX77*$^{+/+}$, data not shown) cortex at E12.5 with no obvious difference in the intensity of label between the different genotypes (Fig. 7A,B). In wild-type embryos at E16.5, Ephrin B2 is strongly expressed in a caudal domain of the neocortex (up to the arrowhead in Fig. 7C). This caudal domain of strong expression of Ephrin B2 is present in the cortex of *PAX77*$^{+}$ (and *PAX77*$^{+/+}$, data not shown) embryos and does not appear contracted (Fig. 7D). In wild-type embryos at E18.5, *Id2* is strongly expressed in a rostral domain in layers 2 and 3 of the neocortex (Fig. 7E, arrow marks the limit of this domain) and in a caudal domain in layer 5 (Fig. 7E, white arrowhead marks the boundary of this domain). These patterns were not altered in *PAX77*$^{+}$ (data not shown) nor in *PAX77*$^{+/+}$ embryos (Fig. 7F).

Cortical areas are also characterized by the specific connections they establish with the thalamus. The somatosensory and visual cortical areas normally establish axonal connexions with the thalamic ventro-posterior geniculate (VP) and dorsal lateral geniculate (dLG), respectively. We examined the organization of thalamocortical projections by injecting fluorescent carbocyanine dyes (DiA and DiI) into visual and somatosensory cortical areas at E17.5 (see Fig. S3A in the supplementary material). Neither *PAX77*$^{+}$ (see Fig. S3C in the supplementary material) nor *PAX77*$^{+/+}$ (data not shown) embryos showed any consistent differences in projections from that of wild type (see Fig. S3B in the supplementary material) and in neither wild-type nor mutant mice did DiA at the caudal pole back label neurons in the VP.

As an additional assay to analyze cortical regionalization in PAX77 mice, we used serotonin-transporter immunostaining on tangential sections through flattened cortices of P7 wild-type and *PAX77*$^{+/+}$ mice to reveal the primary somatosensory area (S1), visual area (V1) and auditory area (A1) (Fig. 8A). We analyzed the size and position of the postero-medial barrel subfield (PMBSF) - the representation of large facial whiskers in the primary somatosensory area. We arbitrarily chose a barrel in the centre of the PMBSF, barrel c4, and determined the ratio between the distance from this barrel to the rostral pole of the cortex (R) and the total length of the cortex (T) (Fig. 8B). This rostral ratio was unchanged in the cortex of PAX77 mice compared to wild type (Fig. 8B). The ratio between the distance of barrel c4 to the caudal pole of the cortex (C) and the total length of the cortex was also unaltered in PAX77 mice compared to wild type (Fig. 8C). We did find, however, that the area of PMBSF relative to the total cortical area was reduced in the PAX77 cortex (Fig. 8D). Thus, although there is no evidence that the overexpression of *Pax6* results in a caudal shift of the somatosensory area, it does reduce its area.

DISCUSSION

Our results show that the *Pax6* gene negatively autoregulates its expression, that increased levels of Pax6 protein cause cell-autonomous proliferative defects of the progenitors that generate the superficial cortical layers and that Pax6 overexpression has surprisingly little effect on cortical arealization. The transgenic model used to make these findings has several major advantages. First, Pax6 levels are not raised excessively, but remain close to physiological levels. Second, Pax6 is not ectopically expressed at sites where Pax6 is not normally found, which would severely complicate the interpretation of abnormalities. Third, the Pax6 protein produced by the transgene has been proven to be functional by genetic complementation (Schedl et al., 1996).

Negative autoregulation of Pax6

Negative feedback is an important component of many stable systems, both biological and non-biological: results from mathematical models and engineered gene circuits have indicated that genes regulated by negative feedback show more stable expression than genes that are unregulated (Hasty et al., 2002). Our identification of negative feedback in the regulation of Pax6 expression in the developing brain highlights the probable importance of maintaining appropriate levels of expression in the face of rapid intra- and extra-cellular changes as embryos grow in size and complexity.

Our evidence for negative autoregulation of an intact locus in vivo comes from the finding that GFP production from the Y1123 transgene, which reports faithfully the sites and levels of activation of *Pax6* (Kleinjan et al., 2006; Tyas et al., 2006), is upregulated on a *Pax6*$^{-/-}$ background, where no endogenous Pax6 or Pax6(5a) protein is present (so freeing reporter expression from regulation), and is reduced in PAX77 embryos in which Pax6 levels are increased. Furthermore, we show that mouse *Pax6* mRNA levels are reduced in mice that

overexpress PAX6. This finding complements nicely previous studies reporting an increased signal from in situ hybridizations for *Pax6* mRNA in the telencephalon of *Pax6*$^{-/-}$ mutants (Muzio et al., 2002) and increased expression of *Pax6* in *Pax6(5a)*$^{-/-}$ mutants (Haubst et al., 2004).

Despite negative feedback, Pax6 protein levels are elevated in PAX77 embryos; thus, negative autoregulation is not able to overcome the effects of introducing five to seven additional copies of the *PAX6* locus in PAX77 mice. We found evidence that it constrains the elevation of Pax6 levels in these mice. Western blots showed that absolute levels of Pax6 proteins are increased in the brain of *PAX77*$^{+}$ embryos by approximately 1.5- to 3-fold. Because *PAX77*$^{+}$ mice contain five to seven extra copies of the gene (seven to nine copies in total, as opposed to two), a slightly larger (3.5- to 4.5-fold) increase in protein levels might have been predicted if each extra copy were functioning at a wild-type level. That they are not is demonstrated by the reduction in expression from the Y1123 transgene on a PAX77 background, which is roughly halved (Fig. 2).

These findings indicate that a negative-feedback mechanism is in place to stabilize Pax6 protein levels. Previous in vitro studies have shown that Pax6 proteins can bind to isolated *Pax6*-promoter sequences, but that this results in activation of transcription (Aota et al., 2003; Okladnova et al., 1998; Plaza et al., 1993; Plaza et al., 1995). Further evidence for such activation comes from in vivo studies showing that, in some tissues (e.g. lens and olfactory placodes, but not in cortex), Pax6 protein is required for transcription of the *Pax6* gene (Aota et al., 2003; Grindley et al., 1995; Kim and Lauderdale, 2006; Kleinjan et al., 2004). The mechanisms regulating the levels of expression of Pax6 are likely to be complex. Our findings implicate negative autoregulation, be it direct or indirect, as a potent stabilizing component in vivo.

Pax6 overexpression affects late cortical progenitor proliferation cell autonomously

We showed that controlled overexpression of Pax6 in vivo specifically affects the proliferation of late cortical progenitors. This effect is strongest in rostral and central parts of the cortex, where levels of Pax6 are highest. At E15.5, there are significant reductions in the proportions of progenitor cells in S-phase and in their densities in M-phase both rostrally and centrally; reductions are slightly greater rostrally. In E16.5 chimeras, there are significant reductions in the numbers of mutant cells in rostral and central proliferative layers; again, the reduction is slightly larger rostrally. In addition, the proportion of mutant cortical progenitors in M-phase in the rostral cortex of the chimeras is lower than normal. Consistent with these findings, superficial cortical layers II-IV, which arise mainly from E15.5 onwards (Gillies and Price, 1993), are significantly thinner in the rostral and central cortex of postnatal Pax6-overexpressing mice. Our in vivo findings complement a previous study reporting that overexpression of Pax6 in vitro by viral transduction of dissociated cortical cells at E14.5 results in an early exit from the cell cycle (Heins et al., 2002).

In E15.5 caudal cortex, where Pax6 levels are lowest, there are no differences in the proportions of progenitor cells in S-phase and their densities in M-phase between PAX77 and wild-type mice. In the caudal cortex of E16.5 chimeras, however, the numbers of mutant cells in the proliferative layers are significantly reduced, although the extent of the reduction is smaller than in central and rostral regions. A possible explanation for these regional differences is that the rostral cortex is more advanced than the caudal cortex at each embryonic age (Bayer and Altman, 1991) and so the emergence of defects in the caudal proliferative layers is delayed.

The emergence of defects occurring earliest in the rostral proliferative layers can explain why defects of mutant cell numbers are restricted to specifically the rostral IZ of E16.5

chimeras (Fig. 4D). These defects have not translated into reductions in mutant cell numbers in the cortical plate by E16.5 (although there was a hint that a defect might be emerging in the rostral cortical plate: Fig. 4E). They are, however, translated into defects of superficial-layer thickness by P7, although we only observed significant reductions rostrally and centrally. Because P7 is after the time at which migration of postmitotic neurons into the cortex is complete both rostrally and caudally, the most likely explanation for the lack of significant thinning caudally is that proliferation is affected less severely here, where Pax6 is expressed at its lowest levels. Overall, our findings indicate that the level of Pax6 within cortical progenitors becomes important in the regulation of their proliferation and hence in the production of cortical layers.

Overexpression of Pax6 has little effect on cortical regionalization

Previous studies have suggested that Pax6 plays an important role in regulating cortical regionalization by promoting rostro-lateral identities and repressing the expression of Emx2, which confers caudo-medial identities (Bishop et al., 2000; Bishop et al., 2002; Muzio et al., 2002; Muzio and Mallamaci, 2003). We predicted that an 1.5- to 3-fold overexpression of Pax6 in the cortex would result in a downregulation of Emx2, such that caudal levels would decrease to the very low levels normally found rostrally, and in a caudal shift of rostral areas (Fig. 6). Unexpectedly, we found unaltered expression of Emx2 in the cortex of PAX77 embryos. The analysis of the expression of cortical markers, the topography of thalamocortical connections and the position of the barrel field did not reveal any difference between wild-type and PAX77 mice, suggesting that cortical regionalization is largely unaffected by Pax6 overexpression. The only defect we observed is a reduction in the size of PMBSF in PAX77 mice.

Previous studies have shown that the loss of Pax6 results in the upregulation of *Emx2* expression (Muzio et al., 2002). One possibility to explain both this previous finding and our new result is that Pax6 is needed to permit the repression of *Emx2*, but that its level of expression does not determine the level of *Emx2* expression. Existing evidence indicates that the loss of Emx2 and overexpression of Emx2 in vivo shift cortical areas either caudally or rostrally, respectively (Bishop et al., 2000; Hamasaki et al., 2004; Muzio et al., 2002). It seems likely that Emx2 plays a dominant role in determining cortical arealization, whereas Pax6 might have little or no direct role. Increased expression of Pax6 might not affect arealization because it has little, if any, effect on Emx2 levels. Loss of Pax6 might indirectly result in a rostral shift of cortical areas (Bishop et al., 2000; Muzio et al., 2002) as consequence of the upregulation of Emx2. However, there are other ways in which the loss of Pax6 might indirectly affect cortical arealization. The reduction of rostro-lateral cortical areas in *Pax6*$^{-/-}$ embryos could be a consequence of the absence of olfactory placodes, which emerge at E9.5 and are a region of mesenchymal-epithelial induction orchestrating regional differentiation and pathway formation in the forebrain (Anchan et al., 1997; Balmer and LaMantia, 2005; LaMantia, 1999; LaMantia et al., 2000; LaMantia et al., 1993). Olfactory placodes fail to form in *Pax6*$^{-/-}$ embryos (Hogan et al., 1986) and the consequent loss of signalling molecules might influence the development and regionalization of the cortex. The olfactory placodes form normally in PAX77 mice (see Fig. S4 in the supplementary material), which might explain the absence of cortical regionalization defects.

On the other hand, we can not altogether exclude the possibility that increasing cortical Pax6 levels does have some effect on cortical arealization. The reduction in the size of the primary somatosensory area in PAX77 mice could reflect the opposing effects of an upregulated Pax6 gradient and an unaffected Emx2 gradient compressing the somatosensory cortex between them, or might result from the increased steepness of the Pax6 gradient. It is also possible, however, that the reduction in size of the somatosensory cortex in PAX77

mice is a consequence of defects in the development of cortical layers II-IV, as discussed above.

Supplementary Material

Refer to Web version on PubMed Central for supplementary material.

Acknowledgments

We thank Simon Saule for the anti-Pax6 antibody; Georgio Corte for the Emx2 antibody; and Dennis O'Leary for the *Id2* in situ probe. We thank Peter Kind and Mark Barnett for advice and technical help with PMBSF labelling and measurements; Mark Barnett for help with qRT-PCR; and Judy Fantes for help with FISH genotyping. We thank Jean Flockhart, Duncan McNeil and Linda Wilson for technical assistance. Research in the authors' laboratory is supported by the Wellcome Trust, the MRC and the BBSRC. M.M. was supported by postdoctoral fellowships from the Association pour la Recherche sur le Cancer (ARC) and the EMBO.

References

Anchan RM, Drake DP, Haines CF, Gerwe EA, LaMantia AS. Disruption of local retinoid-mediated gene expression accompanies abnormal development in the mammalian olfactory pathway. J. Comp. Neurol. 1997; 379:171–184. [PubMed: 9050783]

Aota S, Nakajima N, Sakamoto R, Watanabe S, Ibaraki N, Okazaki K. Pax6 autoregulation mediated by direct interaction of Pax6 protein with the head surface ectoderm-specific enhancer of the mouse Pax6 gene. Dev. Biol. 2003; 257:1–13. [PubMed: 12710953]

Balmer CW, Lamantia AS. Noses and neurons: Induction, morphogenesis, and neuronal differentiation in the peripheral olfactory pathway. Dev. Dyn. 2005; 234:464–481. [PubMed: 16193510]

Bayer SA, Altman J. Development of the endopiriform nucleus and the claustrum in the rat brain. Neuroscience. 1991; 45:391–412. [PubMed: 1762685]

Bishop KM, Goudreau G, O'Leary DD. Regulation of area identity in the mammalian neocortex by Emx2 and Pax6. Science. 2000; 288:344–349. [PubMed: 10764649]

Bishop KM, Rubenstein JL, O'Leary DD. Distinct actions of Emx1, Emx2, and Pax6 in regulating the specification of areas in the developing neocortex. J. Neurosci. 2002; 22:7627–7638. [PubMed: 12196586]

Caric D, Gooday D, Hill RE, McConnell SK, Price DJ. Determination of the migratory capacity of embryonic cortical cells lacking the transcription factor Pax-6. Development. 1997; 124:5087–5096. [PubMed: 9362466]

Carriere C, Plaza S, Martin P, Quatannens B, Bailly M, Stehelin D, Saule S. Characterization of quail Pax-6 (Pax-QNR) proteins expressed in the neuroretina. Mol. Cell. Biol. 1993; 13:7257–7266. [PubMed: 8246948]

Englund C, Fink A, Lau C, Pham D, Daza RA, Bulfone A, Kowalczyk T, Hevner RF. Pax6, Tbr2, and Tbr1 are expressed sequentially by radial glia, intermediate progenitor cells, and postmitotic neurons in developing neocortex. J. Neurosci. 2005; 25:247–251. [PubMed: 15634788]

Estivill-Torrus G, Pearson H, van Heyningen V, Price DJ, Rashbass P. Pax6 is required to regulate the cell cycle and the rate of progression from symmetrical to asymmetrical division in mammalian cortical progenitors. Development. 2002; 129:455–466. [PubMed: 11807037]

Gillies K, Price DJ. Cell migration and subplate loss in explant cultures of murine cerebral cortex. NeuroReport. 1993; 4:911–914. [PubMed: 8369482]

Grindley JC, Davidson DR, Hill RE. The role of Pax-6 in eye and nasal development. Development. 1995; 121:1433–1442. [PubMed: 7789273]

Grindley JC, Hargett LK, Hill RE, Ross A, Hogan BL. Disruption of PAX6 function in mice homozygous for the Pax6Sey-1Neu mutation produces abnormalities in the early development and regionalization of the diencephalon. Mech. Dev. 1997; 64:111–126. [PubMed: 9232602]

Hamasaki T, Leingartner A, Ringstedt T, O'Leary DD. EMX2 regulates sizes and positioning of the primary sensory and motor areas in neocortex by direct specification of cortical progenitors. Neuron. 2004; 43:359–372. [PubMed: 15294144]

Europe PMC Funders Author Manuscripts

Hasty J, McMillen D, Collins JJ. Engineered gene circuits. Nature. 2002; 420:224–230. [PubMed: 12432407]

Haubst N, Berger J, Radjendirane V, Graw J, Favor J, Saunders GF, Stoykova A, Gotz M. Molecular dissection of Pax6 function: the specific roles of the paired domain and homeodomain in brain development. Development. 2004; 131:6131–6140. [PubMed: 15548580]

Heins N, Malatesta P, Cecconi F, Nakafuku M, Tucker KL, Hack MA, Chapouton P, Barde YA, Gotz M. Glial cells generate neurons: the role of the transcription factor Pax6. Nat. Neurosci. 2002; 5:308–315. [PubMed: 11896398]

Hill RE, Favor J, Hogan BL, Ton CC, Saunders GF, Hanson IM, Prosser J, Jordan T, Hastie ND, van Heyningen V. Mouse small eye results from mutations in a paired-like homeobox-containing gene. Nature. 1991; 354:522–525. [PubMed: 1684639]

Hogan BL, Horsburgh G, Cohen J, Hetherington CM, Fisher G, Lyon MF. Small eyes (Sey): a homozygous lethal mutation on chromosome 2 which affects the differentiation of both lens and nasal placodes in the mouse. J. Embryol. Exp. Morphol. 1986; 97:95–110. [PubMed: 3794606]

Keighren M, West JD. Analysis of cell ploidy in histological sections of mouse tissues by DNA-DNA in situ hybridization with digoxigenin-labelled probes. Histochem. J. 1993; 25:30–44. [PubMed: 8432662]

Kerszberg M. Morphogen propagation and action: towards molecular models. Semin. Cell Dev. Biol. 1999; 10:297–302. [PubMed: 10441543]

Kim J, Lauderdale JD. Analysis of Pax6 expression using a BAC transgene reveals the presence of a paired-less isoform of Pax6 in the eye and olfactory bulb. Dev. Biol. 2006; 292:486–505. [PubMed: 16464444]

Kleinjan DA, Seawright A, Childs AJ, van Heyningen V. Conserved elements in Pax6 intron 7 involved in (auto)regulation and alternative transcription. Dev. Biol. 2004; 265:462–477. [PubMed: 14732405]

Kleinjan DA, Seawright A, Mella S, Carr CB, Tyas DA, Simpson TI, Mason JO, Price DJ, van Heyningen V. Long-range downstream enhancers are essential for Pax6 expression. Dev. Biol. 2006; 299:563–581. [PubMed: 17014839]

Kroll TT, O'Leary DD. Ventralized dorsal telencephalic progenitors in Pax6 mutant mice generate GABA interneurons of a lateral ganglionic eminence fate. Proc. Natl. Acad. Sci. USA. 2005; 102:7374–7379. [PubMed: 15878992]

LaMantia AS. Forebrain induction, retinoic acid, and vulnerability to schizophrenia: insights from molecular and genetic analysis in developing mice. Biol. Psychiatry. 1999; 46:19–30. [PubMed: 10394471]

LaMantia AS, Colbert MC, Linney E. Retinoic acid induction and regional differentiation prefigure olfactory pathway formation in the mammalian forebrain. Neuron. 1993; 10:1035–1048. [PubMed: 8318228]

LaMantia AS, Bhasin N, Rhodes K, Heemskerk J. Mesenchymal/epithelial induction mediates olfactory pathway formation. Neuron. 2000; 28:411–425. [PubMed: 11144352]

Lo CW. Localization of low abundance DNA sequences in tissue sections by in situ hybridization. J. Cell Sci. 1986; 81:143–162. [PubMed: 3733894]

Lo CW, Coulling M, Kirby C. Tracking of mouse cell lineage using microinjected DNA sequences: analyses using genomic Southern blotting and tissue-section in situ hybridizations. Differentiation. 1987; 35:37–44. [PubMed: 3428512]

Mallamaci A, Di Blas E, Briata P, Boncinelli E, Corte G. OTX2 homeoprotein in the developing central nervous system and migratory cells of the olfactory area. Mech. Dev. 1996; 58:165–178. [PubMed: 8887325]

Mallamaci A, Iannone R, Briata P, Pintonello L, Mercurio S, Boncinelli E, Corte G. EMX2 protein in the developing mouse brain and olfactory area. Mech. Dev. 1998; 77:165–172. [PubMed: 9831645]

Martynoga B, Morrison H, Price DJ, Mason JO. Foxg1 is required for specification of ventral telencephalon and region-specific regulation of dorsal telencephalic precursor proliferation and apoptosis. Dev. Biol. 2005; 283:113–127. [PubMed: 15893304]

Mastick GS, Davis NM, Andrew GL, Easter SS Jr. Pax-6 functions in boundary formation and axon guidance in the embryonic mouse forebrain. Development. 1997; 124:1985–1997. [PubMed: 9169845]

Muzio L, DiBenedetto B, Stoykova A, Boncinelli E, Gruss P, Mallamaci A. Emx2 and Pax6 control regionalization of the pre-neuronogenic cortical primordium. Cereb. Cortex. 2002; 12:129–139. [PubMed: 11739261]

Muzio L, Mallamaci A. Emx1, emx2 and pax6 in specification, regionalization and arealization of the cerebral cortex. Cereb. Cortex. 2003; 13:641–647. [PubMed: 12764040]

Neumann C, Cohen S. Morphogens and pattern formation. BioEssays. 1997; 19:721–729. [PubMed: 9264255]

Okladnova O, Syagailo YV, Mossner R, Riederer P, Lesch KP. Regulation of PAX-6 gene transcription: alternate promoter usage in human brain. Brain Res. Mol. Brain Res. 1998; 60:177–192. [PubMed: 9757029]

Pinson J, Simpson TI, Mason JO, Price DJ. Positive autoregulation of the transcription factor Pax6 in response to increased levels of either of its major isoforms, Pax6 or Pax6(5a), in cultured cells. BMC Dev. Biol. 2006; 6:25. [PubMed: 16725027]

Plaza S, Dozier C, Saule S. Quail Pax-6 (Pax-QNR) encodes a transcription factor able to bind and trans-activate its own promoter. Cell Growth Differ. 1993; 4:1041–1050. [PubMed: 8117618]

Plaza S, Dozier C, Turque N, Saule S. Quail Pax-6 (Pax-QNR) mRNAs are expressed from two promoters used differentially during retina development and neuronal differentiation. Mol. Cell. Biol. 1995; 15:3344–3353. [PubMed: 7760830]

Porteus MH, Brice AE, Bulfone A, Usdin TB, Ciaranello RD, Rubenstein JL. Isolation and characterization of a library of cDNA clones that are preferentially expressed in the embryonic telencephalon. Brain Res. Mol. Brain Res. 1992; 12:7–22. [PubMed: 1372074]

Pratt T, Vitalis T, Warren N, Edgar JM, Mason JO, Price DJ. A role for Pax6 in the normal development of dorsal thalamus and its cortical connections. Development. 2000; 127:5167–5178. [PubMed: 11060242]

Pratt T, Tian NM, Simpson TI, Mason JO, Price DJ. The winged helix transcription factor Foxg1 facilitates retinal ganglion cell axon crossing of the ventral midline in the mouse. Development. 2004; 131:3773–3784. [PubMed: 15240555]

Quinn JC, Molinek M, Martynoga BS, Zaki PA, Faedo A, Bulfone A, Hevner RF, West JD, Price DJ. Pax6 controls cerebral cortical cell number by regulating exit from the cell cycle and specifies cortical cell identity by a cell autonomous mechanism. Dev. Biol. 2006 doi:10.1016/j.physletb.2003.10.071.

Rubenstein JL, Anderson S, Shi L, Miyashita-Lin E, Bulfone A, Hevner R. Genetic control of cortical regionalization and connectivity. Cereb. Cortex. 1999; 9:524–532. [PubMed: 10498270]

Schedl A, Ross A, Lee M, Engelkamp D, Rashbass P, van Heyningen V, Hastie ND. Influence of PAX6 gene dosage on development: overexpression causes severe eye abnormalities. Cell. 1996; 86:71–82. [PubMed: 8689689]

Schmahl W, Knoedlseder M, Favor J, Davidson D. Defects of neuronal migration and the pathogenesis of cortical malformations are associated with Small eye (Sey) in the mouse, a point mutation at the Pax-6-locus. Acta Neuropathol. 1993; 86:126–135. [PubMed: 8213068]

Schuurmans C, Armant O, Nieto M, Stenman JM, Britz O, Klenin N, Brown C, Langevin LM, Seibt J, Tang H, et al. Sequential phases of cortical specification involve Neurogenin-dependent and -independent pathways. EMBO J. 2004; 23:2892–2902. [PubMed: 15229646]

Stoykova A, Fritsch R, Walther C, Gruss P. Forebrain patterning defects in Small eye mutant mice. Development. 1996; 122:3453–3465. [PubMed: 8951061]

Tabata T, Takei Y. Morphogens, their identification and regulation. Development. 2004; 131:703–712. [PubMed: 14757636]

Tarabykin V, Stoykova A, Usman N, Gruss P. Cortical upper layer neurons derive from the subventricular zone as indicated by Svet1 gene expression. Development. 2001; 128:1983–1993. [PubMed: 11493521]

Tyas DA, Simpson TI, Carr CB, Kleinjan DA, van Heyningen V, Mason JO, Price DJ. Functional conservation of Pax6 regulatory elements in humans and mice demonstrated with a novel transgenic reporter mouse. BMC Dev. Biol. 2006; 6:21. [PubMed: 16674807]

Walther C, Gruss P. Pax-6, a murine paired box gene, is expressed in the developing CNS. Development. 1991; 113:1435–1449. [PubMed: 1687460]

Warren N, Price DJ. Roles of Pax-6 in murine diencephalic development. Development. 1997; 124:1573–1582. [PubMed: 9108373]

Watson RF, Abdel-Majid RM, Barnett MW, Willis BS, Katsnelson A, Gillingwater TH, McKnight GS, Kind PC, Neumann PE. Involvement of protein kinase A in patterning of the mouse somatosensory cortex. J. Neurosci. 2006; 26:5393–5401. [PubMed: 16707791]

West JD, Flockhart JH. Genotypically unbalanced diploid<==>diploid foetal mouse chimaeras: possible relevance to human confined mosaicism. Genet Res. 1994; 63:87–99. [PubMed: 8026741]

Yucel G, Small S. Morphogens: precise outputs from a variable gradient. Curr. Biol. 2006; 16:R29–R31. [PubMed: 16401416]

Europe PMC Funders Author Manuscripts

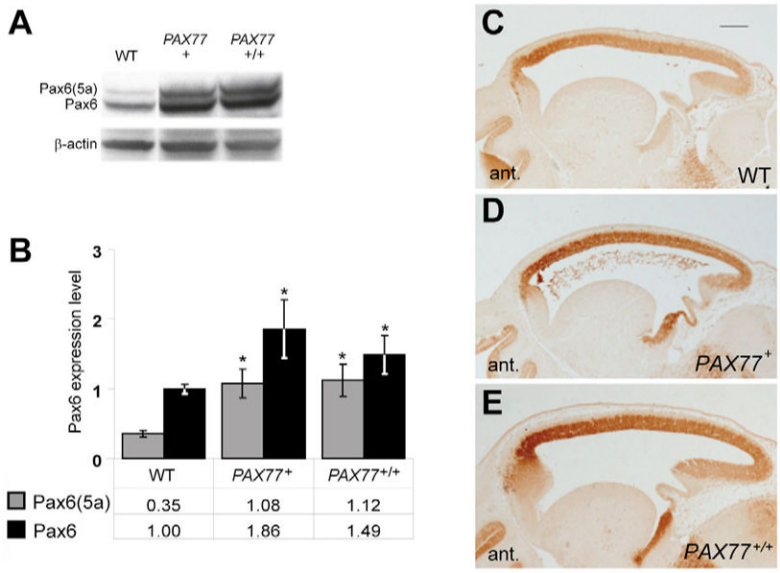

Fig. 1. Pax6 protein levels are increased in PAX77 mice

(**A**) Western-blots of E12.5 wild-type, *PAX77*$^{+}$ and *PAX77*$^{+/+}$ telencephalic-protein extracts with anti-Pax6 and anti-β-actin antibodies. (**B**) Quantitation of the two isoforms, 48 kDa Pax6(5a) and 46 kDa Pax6, in E12.5 wild-type *PAX77*$^{+}$ and *PAX77*$^{+/+}$ telencephalons. For each sample, the intensity of the Pax6 and Pax6(5a) bands was divided by the intensity of the β-actin band to account for loading differences and values were calculated relative to the mean value for wild-type Pax6, which was assigned a value of 1 (mean±s.e.m. are shown; n=3 in all cases). Asterisks indicate statistically significant differences from wild type (Student's t-test, P<0.05). There was no significant difference between the levels of Pax6 and Pax6(5a) in *PAX77*$^{+/+}$ and *PAX77*$^{+}$ embryonic brains. (**C-E**) Immunohistochemistry on sagittal sections through the cortex showing Pax6 expression in (C) wild-type (WT), (D) *PAX77*$^{+}$ and (E) *PAX77*$^{+/+}$ E12.5 embryos. The rostro-lateral^{high} to caudo-medial^{low} gradient of Pax6 expression is conserved in the cortex of PAX77 mice. Scale bar: 200 μm.

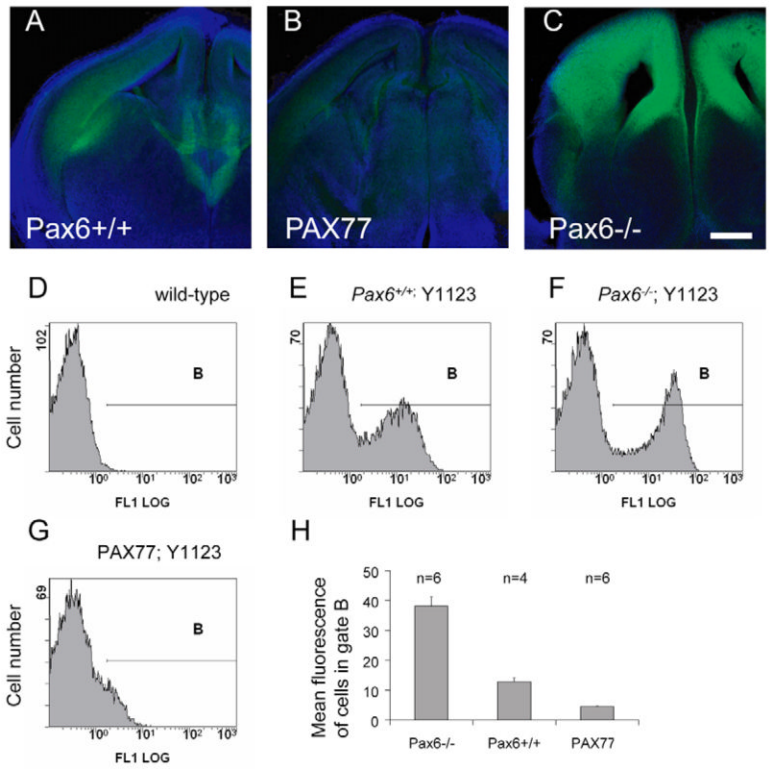

Fig. 2. Telencephalic expression of tau-GFP from Y1123 is regulated by differences in the levels of Pax6 expression

Expression is shown in coronal sections from (**A**) *Pax6*$^{+/+}$, (**B**) PAX77 and (**C**) *Pax6*$^{-/-}$ E14.5 embryos. Scale bar: 200 μm. (**D-H**) Expression of tau-GFP quantified with flow cytometry. (D-G) Examples of frequency histograms of cell number against GFP fluorescence for samples of cells from the brains of (D) wild-type embryos and (E-G) embryos containing Y1123 on (E) a wild-type background, (F) a *Pax6*$^{-/-}$ background and (G) a PAX77 background. (H) Histogram showing the mean fluorescence of cells in gate B (see D-G) from four to six embryos with each Y1123-containing genotype. All differences are significant (P<0.001; Student's t-test).

Europe PMC Funders Author Manuscripts

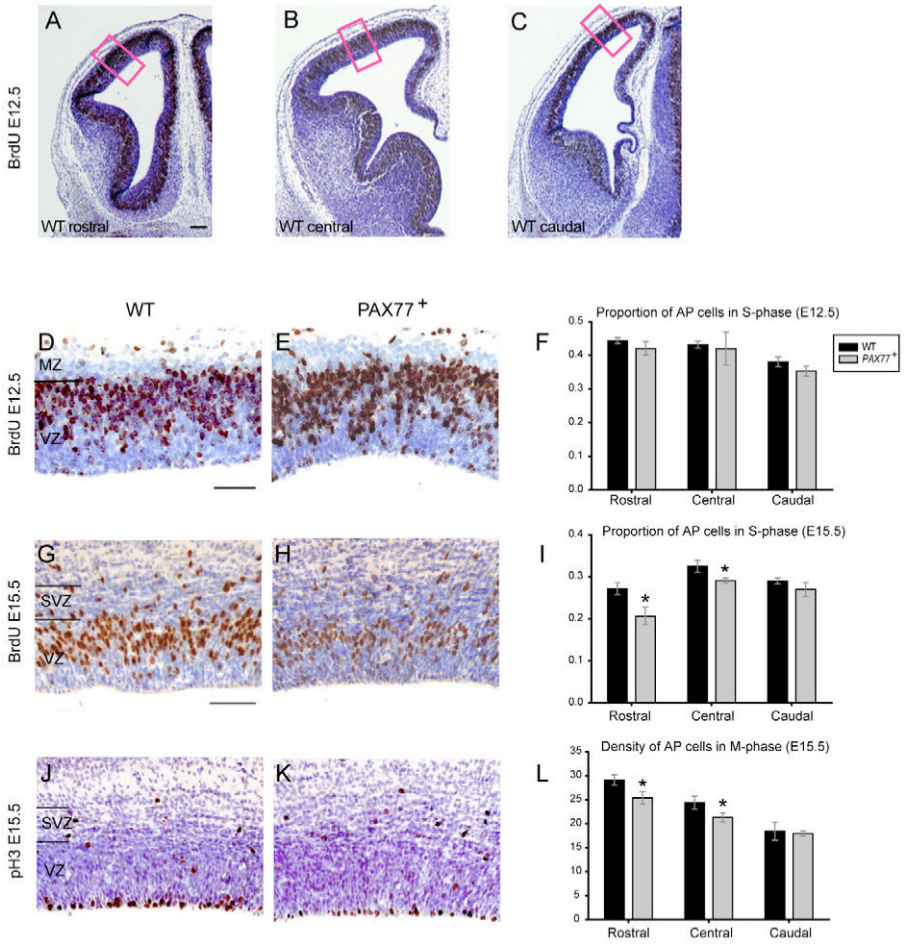

Fig. 3. Pax6 overexpression affects late cortical progenitor proliferation

(**A-C**) Coronal sections at (A) rostral, (B) central and (C) caudal levels of the cortex (left hemisphere shown) of an E12.5 wild-type embryo labeled with anti-BrdU (brown). Cell counts were made in 100 μm-wide sampling boxes (red boxes). (**D**,**E**) Examples of anti-BrdU labelling (brown) of coronal sections of the cortex of (D) a wild-type and (E) a PAX77 embryo at E12.5. (**F**) The proportion of AP cells in S-phase along the cortex of PAX77 embryos at E12.5 is not different from that of wild type. (**G**,**H**) Example of anti-BrdU labeling (brown) of coronal sections of the cortex of (G) a wild-type and (H) a PAX77 embryo at E15.5. (**I**) The proportion of AP cells in S-phase in the rostral and central cortex of PAX77 embryos at E15.5 is significantly decreased compared with wild type. (**J**,**K**) Example of anti-phosphorylated histone H3 labeling (brown) of coronal sections of the cortex of (J) a wild-type and (K) a PAX77 embryo at E15.5. (**L**) The density of AP cells in M-phase in the rostral and central cortex of PAX77 embryos at E15.5 is significantly decreased compared with wild type. All sections shown are counterstained with cresyl violet. MZ, marginal zone; VZ, ventricular zone; SVZ, subventricular zone. Scale bars: 50 μm in A-E, 70 μm in G,H,J,K.

Europe PMC Funders Author Manuscripts

Europe PMC Funders Author Manuscripts

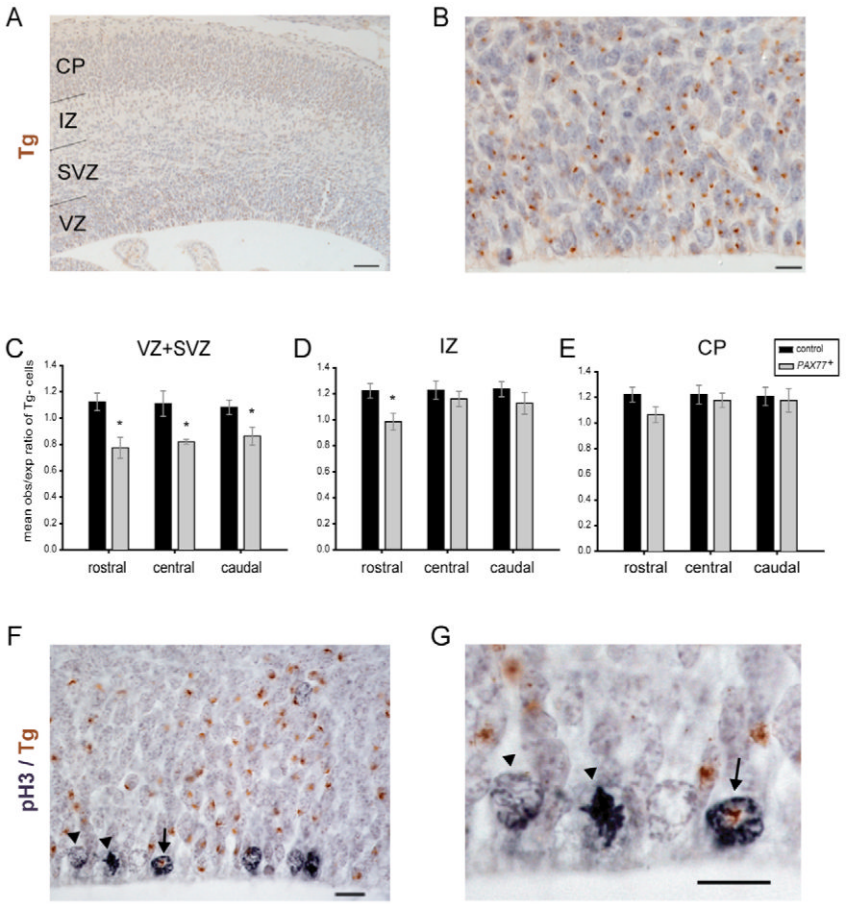

Fig. 4. PAX77 cells are under-represented in the cortical proliferative layers of *PAX77*$^{+}$;Tg^{-}↔wild-type;Tg^{+} chimeric embryos at E16.5

(A,B,F,G) Coronal sections through the cortex of a *PAX77*$^{+}$;Tg^{-}↔wild-type;Tg^{+} chimera at E16.5. (**A**,**B**) Tg^{+} cells (marked with brown dots) and Tg^{-} cells were counted in the proliferative layers (VZ and SVZ), intermediate zone (IZ) and cortical plate (CP). (**C-E**) Ratios of observed/expected contributions of Tg^{-} (i.e. PAX77) cells in (C) VZ and SVZ, (D) IZ and (E) CP. (C) PAX77;Tg^{-} cells are significantly under-represented in the proliferative layers along the chimeric cortex and (D) in the IZ of the rostral chimeric cortex. (**F**,**G**) Example of Tg^{+} (arrow) and Tg^{-} (arrowhead) apical progenitors in M-phase labelled with anti-phosphorylated histone H3 (grey). Scale bars: 50 μm in A; 10 μm in B,F,G.

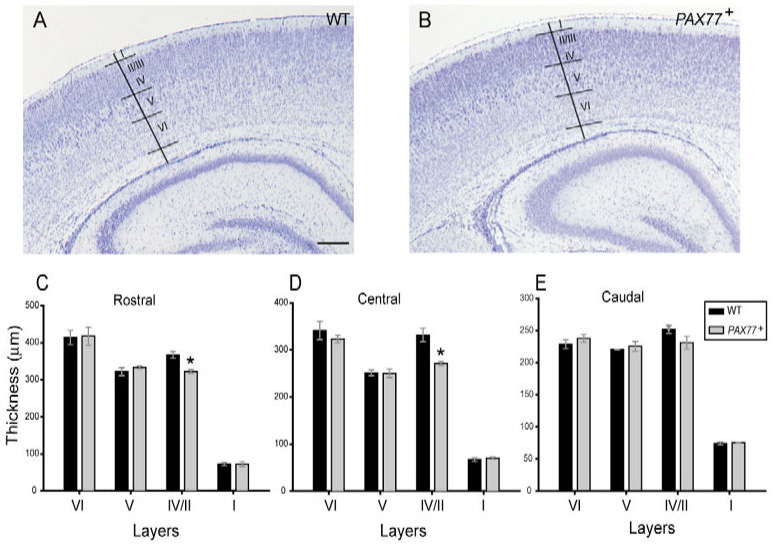

Fig. 5. Pax6 overexpression affects the formation of superficial cortical layers

(**A**,**B**) Coronal sections through the cortex of (A) a wild-type and (B) a PAX77 mouse at P7, stained with cresyl violet. Borders between adjacent cortical layers were identified based on differences in cytoarchitecture. (**C**-**E**) Thickness of cortical layers I, II-IV (combined), V and VI in the (C) rostral, (D) central and (E) caudal cortex of wild-type and PAX77 mice at P7. The thickness of layers II-IV is significantly decreased in the rostral and central cortex of PAX77 mice compared with wild type. Scale bar: 300 μm.

Europe PMC Funders Author Manuscripts

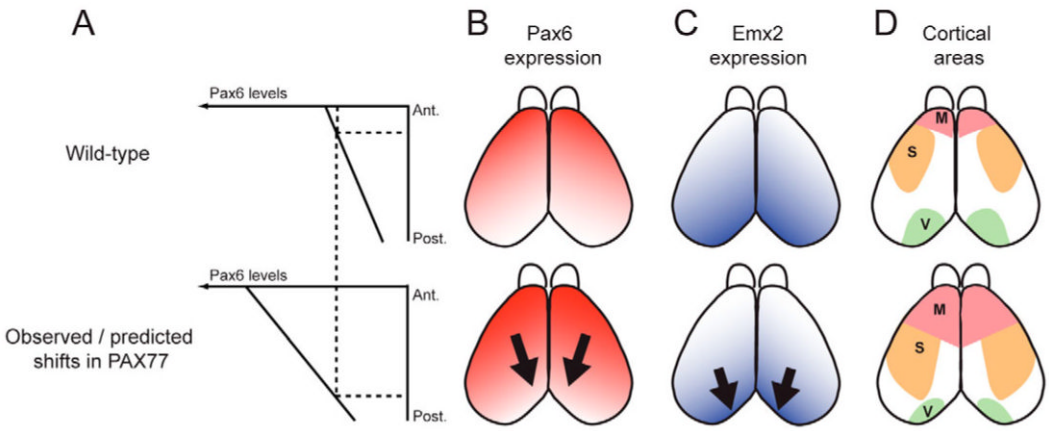

Fig. 6. Predicted shifts in the cortex of PAX77 mice

(**A**) Pax6 levels are about three times higher in the anterior cortex than in the posterior cortex. In PAX77 mice, Pax6 expression is still graded, but is increased by 1.5- to 3-fold (shown here as an average of approximately 2-fold). Thus, in PAX77 embryos, cells in posterior regions of the cortex express levels of Pax6 that are normally found in anterior regions. (**B-D**) Dorsal views of mouse neocortex. (B) In the wild-type, *Pax6* is expressed in a rostro-lateral^{high} to caudo-medial^{low} gradient, while (C) *Emx2* is expressed in an opposite gradient. We predicted that the overexpression of *Pax6* would result in a downregulation of *Emx2* expression and (D) in a caudal shift of rostral areas at the expense of caudal areas. M, motor area; S, somatosensory area; V, visual area.

Europe PMC Funders Author Manuscripts

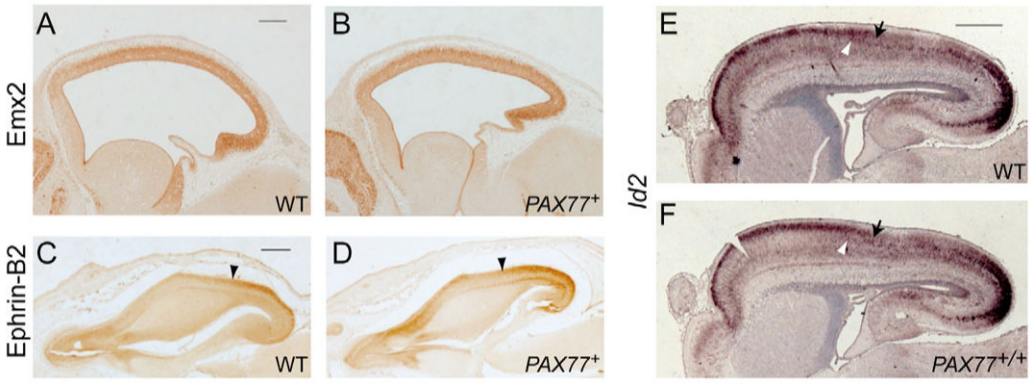

Fig. 7. *Pax6* overexpression does not alter the expression profile of cortical regionalization markers

(**A**,**B**) Immunohistochemistry on sagittal sections through the cortex of (A) wild-type and (B) *PAX77*$^{+}$ E12.5 embryos showing the expression of Emx2. The gradient of Emx2 expression is conserved in the cortex of PAX77 mice and overall levels are not reduced. (**C**,**D**) Immunohistochemistry on horizontal sections through the cortex of (C) wild-type and (D) *PAX77*$^{+}$ E16.5 embryos showing the expression of Ephrin B2 in the right hemisphere. In the wild-type embryo, Ephrin B2 is strongly expressed in a caudal domain (arrowhead shows the anterior limit of the Ephrin B2 caudal expression domain). This caudal domain is present and does not appear contracted in the PAX77 cortex. (**E**,**F**) In situ hybridizations on sagittal sections through the forebrain of (E) wild-type and (F) *PAX77*$^{+/+}$ E18.5 embryos showing the expression of *Id2* mRNA. In the wild-type embryo, *Id2* is strongly expressed in layers 2 and 3 in an anterior domain (black arrow shows the posterior limit of this domain), and in layer 5 in a caudal domain (white arrowhead shows the anterior limit of this domain). The expression of *Id2* appears unaltered in the PAX77 cortex. Scale bars: 200 μm in A-C; 0.5 mm in D-H.

Europe PMC Funders Author Manuscripts

Europe PMC Funders Author Manuscripts

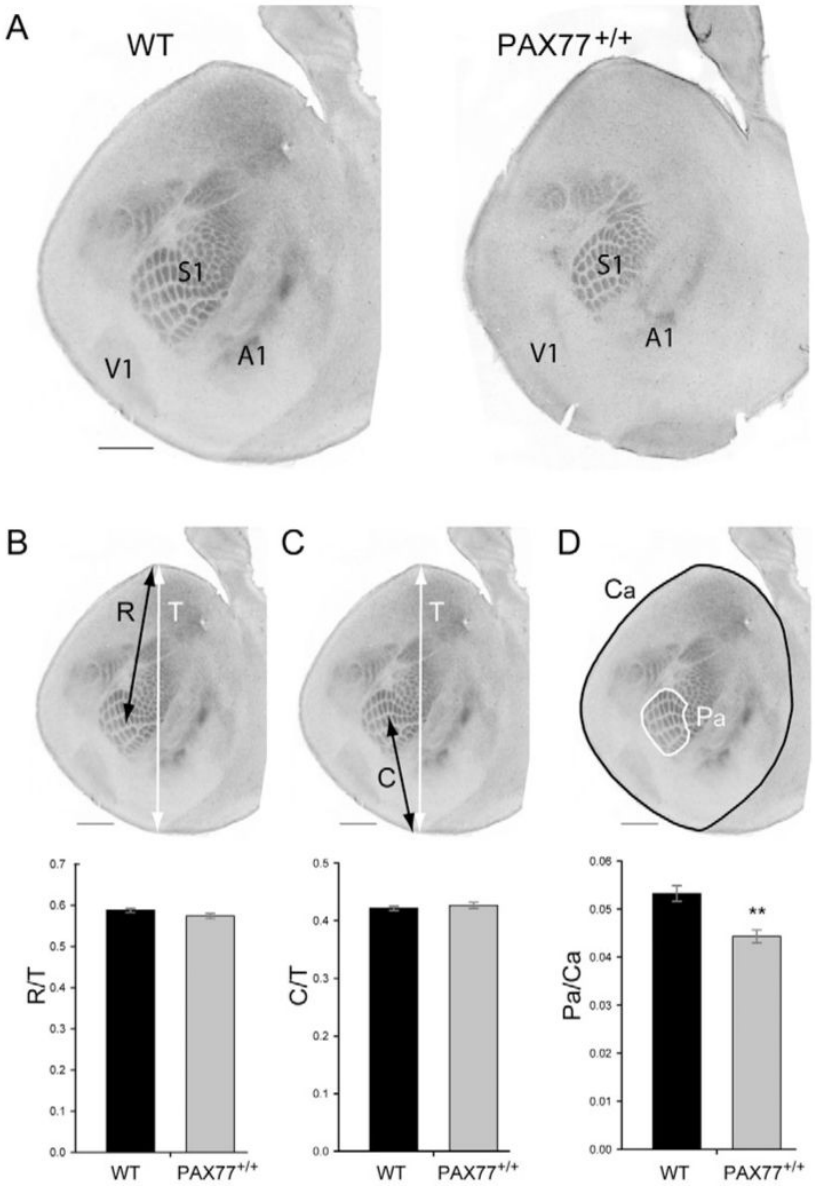

Fig. 8. The position of the postero-medial barrel subfield (PMBSF) is not shifted in PAX77 cortex but its size is reduced

(**A**) Tangential sections through one cortical hemisphere of P7 wild-type and *PAX77*$^{+/+}$ mice stained with anti-serotonin transporter. The primary somatosensory (S1), auditory (A1) and visual (V1) areas are revealed. (**B**) Measurements of the ratio between the distance of barrel c4 from the rostral pole of the cortex (R, black arrow) and the total length of the cortex (T, white arrow). No significant difference was found between wild-type and PAX77 mice (Student's *t*-test, n=16). (**C**) Measurement of the ratio between the distance of barrel c4 from the caudal pole of the cortex (C, black arrow) and the total length of the cortex (T, white arrow). No significant difference was found between wild-type and PAX77 mice (Student's *t*-test, n=16). (**D**) Measurement of the ratio between the area of the PMBSF (Pa) and the total area of the cortex (Ca). **Area of PMBSF relative to the total cortical area was significantly reduced in the PAX77 brain compared with wild type (Student's *t*-test, P<0.01, n=13 wild-type brains and 8 *PAX77*$^{+/+}$ brains). Scale bars: 1 mm.